High-strain-rate superplasticity in oxide ceramics: a trial of microstructural design based on creep-cavitation mechanisms

Keijiro HIRAGA *, *Byung-Nam KIM, Koji MORITA, Hidehiro YOSHIDA, Yoshio SAKKA and Masaaki TABUCHI*

National Institute for Materials Science, 1-2-1, Sengen, Tsukuba-shi, Ibaraki 305-0047, Japan

Manuscript received 1 December 2010; in revised form 29 April 2011

From existing knowledge about high-temperature cavitation mechanisms, necessary conditions were discussed for the suppression of cavitation failure during superplastic deformation in ceramic materials. The discussion, where special attention was placed on the relaxation of stress concentrations during grain-boundary sliding and cavity nucleation and growth, leaded to a conclusion that cavitation failure could be retarded by the simultaneous controlling of the initial grain size, the number of residual defects, diffusivity, dynamic grain growth and the homogeneity of microstructure. On the basis of this conclusion, high-strain-rate superplasticity (defined as superplasticity at a strain rate higher than 0.01 s^{-1}) could be intentionally attained in some oxide ceramic materials. This was shown in tetragonal zirconia and composites consisting of zirconia, α-alumina and a spinel phase.

KEY WORDS Grain-boundary sliding; Accommodation; Stress concentration; Diffusional relaxation; Cavity nucleation; Cavity growth; Dynamic grain growth

1 Introduction

Superplasticity is the ability of a material to show large tensile ductility and provides an attractive route for near net-shape forming and joining of materials. In ceramic materials, this ability was discovered by Wakai *et al.*[1] and succceeding studies demonstrated superplastic bulging[2], forging[3,4], deep drawing and joining[5] in zirconia- and alumina-base materials. However, industrial applications have still been limited, in contrast to superplastic metallic materials[6]. One of the major causes of this situation is the limited strain rate that can be available to superplastic forming. In most ceramics, superplasticity occurs at strain rates around 10^{-4} s^{-1} or lower even at high temperatures in a range of 1400–1650 °C. At a strain rate of 10^{-4} s^{-1}, it takes about three hours to elongate a material having an initial length of 10 mm to a final length of 20 mm. Such a long forming time is unattractive in industry. To overcome this drawback, higher strainrates are necessary: when a strain rate higher than 10^{-2} s^{-1} is possible, the forming time for the above-mentioned example is reduced to shorter than two minutes. Superplasticity at 10^{-2} s^{-1}, namely high-strain-rate superplasticity (HSRS) is thus a key for industrial near net-shaping in ceramic materials.

This paper addresses the conditions necessary for attaining HSRS in oxide ceramics. First, factors limiting the strain rate of superplastic deformation are discussed on the ba-

*Corresponding author. PhD; Tel: +81 298 592538.

E-mail address: HIRAGA.Keijiro@nims.go.jp (Keijiro HIRAGA)

sis of existing knowledge about high-temperature creep deformation and cavitation failure mechanisms in polycrystalline materials. Second, in the light of thediscussion, necessary conditions are extracted for attaining HSRS in oxide materials. Finally, it is demonstrated that microstructural control satisfying the necessaary conditions lead to HSRS in monorithic and composite oxide materials.

2 Factors Limiting the Superplastic Strain Rate

2.1 Creep equation

In ceramic materials of which grains are rigid, the combination of grain-boundary sliding, grain switching and grain rearrangement accommodated by diffusion[7,8] can be regarded as the main mechanism of superplastic deformation. If this combination is ideally uniform and successive, then superplastic deformation is also uniform and successive without cavitation damage along grain boundaries and at multiple junctions. For such an ideal case, the stress-strain rate relationship is given as

$$\dot{\varepsilon} = A\exp(-Q/RT)\sigma^n d^{-p} \tag{1}$$

where $\dot{\varepsilon}$ is the strain rate, A is a material constant, Q is the apparent activation energy, R is the gas constant, T is the deformation temperature, σ is the applied stress, n is the stress exponent, d is the grin size and p is the grain-size exponent. For a fixed combination of stress and temperature, Eq.(1) tells that the strain rate can be heightened by a reduction in the grain size. For example, a grain-size reduction to $0.32d$–$0.46d$ for a typical p value of 2–3 increases the strain rate by a factor of 10. The equation also tells that an increase in the $A\exp(-Q/RT)$ term, which means enhanced diffusion along grain boundaries and/or within grains, heightens the strain rate. Enhanced diffusion is empirically known to occur from the doping of aliovalent cations and relates closely to grain growth[9] and stress concentration and relaxation[10,11] during deformation.

In actual ceramic materials, however, the combination of grain-boundary sliding, grain switching, grain rearrangement and accommodation processes is not ideal. We should also note that Eq.(1) does not consider any microstructural changes during deformation. Experimental studies have shown that superplastic deformation is accompanied by accelerated grain growth (dynamic grain growth)[12,13] and intergranular cavitation[12–20]. The former increases the level of flow stress for a given strain rate and enhances the latter. Since cavitation damage leads to premature failure[12–14,18–21], consideration to these dynamic phenomena is indispensable for attaining HSRS.

2.2 Creep cavity nucleation

Theoretical models for intergranular cavitation[10,11,22] tell that cavity nucleation occurs owing to stress concentrations arising from the inhomogeneity of microstructures and chemical compositions. Even in a monolithic material, there are distributions of grain size, grain shape and chemical composition. For this reason, stress distribution, chemical potential and hence the combination of grain-boundary sliding and grain switching coupled with diffusion also become inhomogeneous in a microscopic scale. There is consequently a finite probability of the breakdown of the accommodation processes, particularly in some localized portions where the geometry and the chemical composition are steeply changed. This means equivalently that in such portions, stress concentrations caused by

grain-boundary sliding cannot always be relaxed sufficiently by diffusion. Typical examples of such portions are multiple grain junctions and phase boundaries, where cavity nuclei have frequently been observed after superplastic deformation (Fig.1).

Although the detailed relationship among diffusion, stress concentrations, stress relaxation and cavity nucleation has not been established yet in superplastic ceramics, estimation[23,24] is possible of the relaxation length, Λ[11], over which grain-boundary diffusion can relax the stressconcentrations caused by deformation. The relaxation length is given as

$$\frac{\Lambda}{d} = \left(\frac{L}{d}\right)^{\frac{1}{[1-s(n-1)/3]}} \tag{2}$$

where L is the characteristic diffusive length given by Eq.(3) and s is the extent of stress singularity at the triple junction in the absence of diffusion

$$L = \left(\frac{\delta D_{\mathrm{b}} \sigma \Omega}{k_{\mathrm{B}} T \dot{\varepsilon}}\right)^{1/3} \tag{3}$$

where $\delta D_{\mathrm{b}} \propto \exp(-Q/RT)$ is the grain-boundary diffusion coefficient, Ω is the atomic volume and k_{B} is the Boltzmann constant.

For an aggregate of a tetrakaidecahedron having a facet length of e=$d/3$ (Fig.2), there are three representatives in the relationship between the relaxation distance and the grain

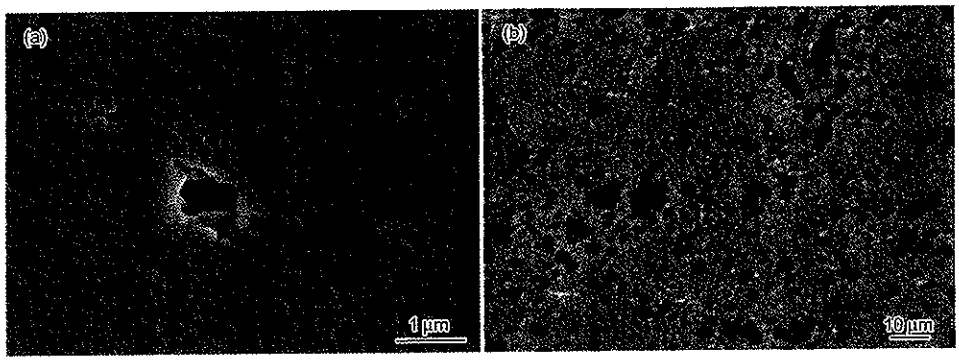

Fig.1 Intergranular cavitation during superplastic tensile deformation in oxide ceramics (tensile axis is horizontal): (a) cavity nucleation at multiple junctions in 3Y-TZP[17]; (b) micrometer-sized cavities grown from cavity nuclei and preexistent defects in ZrO_2-dispersed Al_2O_3[19].

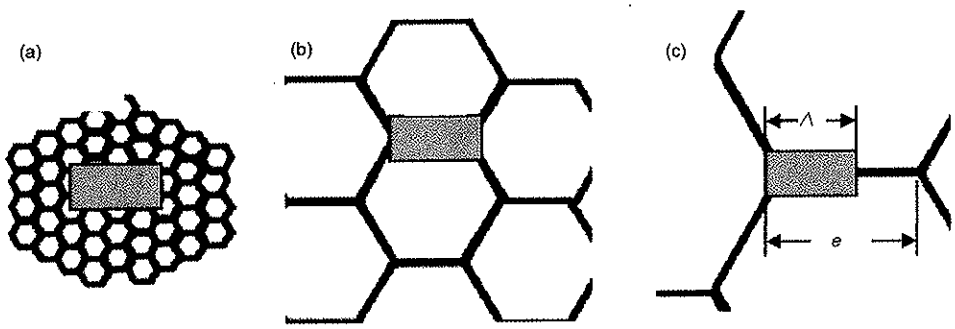

Fig.2 Relatioships between the grain-facet length (e) and the relaxation distance (Λ): (a) Λ>e, (b) Λ=e, (c) Λ<e.

facet length, e: (a) $\Lambda > e$, (b) $\Lambda = e$ and (c) $\Lambda < e$. For (a), stress relaxation is sufficient and consequently cavity nucleation should be suppressed. Cavity nucleation is expected to occur for (c) where relaxation is insufficient. In an extreme case of $\Lambda << e$, instantaneous debonding may occur along grain-boundaries or interfaces. Taking the diffusion data for a Ce-doped tetragonal ZrO_2[25] and an average dihedral angle of 120°, for which s is 0.45, and assuming n=3 and σ=30 MPa, we can calculate the critical situation of (b), for which $d_c = 3e = 3\Lambda$. This calculation gives Fig.3 for T=1400–1500 °C with and without enhanced diffusion[23].

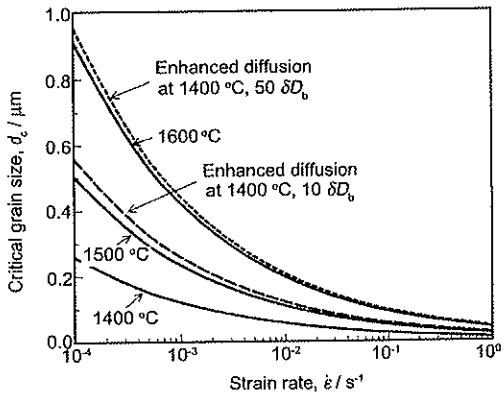

Fig.3 Estimation of the critical grain size over which grain-boundary diffusion can relax stress concentrations caused by grain-boundary sliding.

Fig.3 leads to the following insight into the stress relaxation. First, the critical grain size for a given temperature decreases steeply with an increase in the strain rate. For example, the critical grain size at T=1400 °C is 0.26 μm for ordinary super plasticity at a strain rate of 10^{-4} s^{-1}, whereas the size is reduced to 0.06 μm for HSRS at 10^{-2} s^{-1}. Second, for a fixed grain size, the critical temperature, T_c, above which stress relaxation becomes sufficient, increases with increasing strain rate. For d_c=0.2 μm, T_c increases from 1400 to 1600 °C as the strain rate increases from about 2×10^{-4} to 10^{-2} s^{-1}. Finally, enhanced diffusion increases the critical grain size for a given strain rate. When the grain boundary diffusivity increases by a factor of 50 at 1400 °C, the critical size increases from 0.06 μm to 0.2 μm at 10^{-2} s^{-1}. The estimation also predicts that the enhanced diffusion by factors of 10 and 50 corresponds to increases in the critical temperature by about 100 °C and 200 °C, respectively. For $50\delta D_b$, stress relaxation at 10^{-2}s^{-1} is expected to become sufficient for d=0.2 μm even at 1400 °C. Thus, grain-size reduction, suppressed grain growth and enhanced diffusion are essential for attaining sufficient stress relaxation and suppressed cavity nucleation during high-strain-rate deformation.

The existing models[10,11,22] also predict the following relationship between cavity nucleation and material parameters. The probability of cavity nucleation depends on the grain-boundary diffusivity, the surface energy, γ_s, the grain-boundary energy, γ_b, and geometrical factors such as the dihedral angle between the grain facets. For a fixed grain size, for example, the probability of cavity nucleation decreases with increasing δD_b and γ_s and with decreasing γ_b. In spite of such knowledge about cavity nucleation, information has still been limited on the relationship among these parameters, chemical compositions and minor additives. Recent studies on Y-TZP doped with aliovalent cations for a fixed grain size[26–28] suggest, however, that a first-principle molecular-orbital calculation may give a new aspect to this issue. The studies found a close relationship between tensile ductility and the total bond-overlap population (BOP) that represents the strength of covalent bonding among the constitutive ions: ductility increases with increasing BOP. This result suggests a close relationship between BOP and γ_b and/or γ_s, since tensile ductility should strongly be controlled by the rate of cavity nucleation for a fixed combination of the

major chemical composition, the initial grain size and the loading conditions[23]. The final point about cavity nucleation is the level of flow stress. Since the nucleation rate depends strongly on $\exp(-1/\sigma^2)$[10,11,22], attaining a reduction in the flow stress is of particular importance.

2.3 Creep cavity growth and cracking

During superplastic deformation, nanometer-sized cavity nuclei and defects remaining after sintering grow into micrometer-sized voids (Fig.1b). It has been found in zirconia-base[17] and alumina-base[19,29] materials that the growth of the micrometer-sized voids follows $\mathrm{d}D/\mathrm{d}\varepsilon=\eta D$, where D is the cavity diameter and η is a constant taking a value of about unity. This equation means that the voids are grown by the plastic flow of the material[30]. Such a plastic mechanism is not contradictory to the fact that the grains are rigid, since the aggregate of the rigid grains surrounding the micrometer-sized voids behaves as a plastic body in superplastic ceramics. In the plastic growth mechanism, the increment of void volume during deformation is determined by the increment of plastic strain. Accordingly, the void growth cannot be controlled by the modifications of chemical compositions and microstructure. The growing voids interlink with each other, resulting in cracking in a direction perpendicular to the stress axis[12–14,18–20]. A close resemblance has been found between this process and that of ductile failure in metallic materials containing microvoids or hard inclusions[30]. The cavity growth and cracking processes indicate that reduction in the number of residual defects after sintering and the suppression of cavity nucleation during deformation are essential for suppressing damage accumulation due to void growth.

2.4 Dynamic grain growth

The suppression of dynamic grain growth is necessary for maintaining a lower level of flow stress (Eq.(1)) and a shorter length of grain facet to be relaxed by diffusion (Eq.(2)), both of which are indispensable for the suppression of cavity nucleation. Of the models for dynamic grain growth[31–35], a model derived from a diffusion mechanism[35] may provide a useful insight into this issue, owing to its simplicity in the expression and its agreement with experimental data. The model gives the differential of grain size during deformation as the sum of the dynamic and the static components expressed by the first and second right-hand terms of Eq.(4), respectively:

$$\mathrm{d}d = \alpha d\mathrm{d}\varepsilon + \frac{k}{m}d^{1-m}\mathrm{d}t \tag{4}$$

where α is a constant depending on the grain shape and the grain-size distribution, m and k are the grain-growth exponent and the kinetic constant, respectively, of the static grain-growth law, $d^m - d_0^m=kt$, where t is the heating time. Under an initial condition of $d=d_0$ at $\varepsilon=0$, Eq.(4) yields the following equation for constant displacement-rate loading[19]:

$$d = \left[d_0^m\exp(\alpha m\varepsilon) + \frac{k\{\exp(\varepsilon) - \exp(\alpha m\varepsilon)\}}{\dot{\varepsilon}(1-\alpha m)}\right]^{1/m} \tag{5}$$

Eq.(5) indicates that the grain size for a given strain becomes smaller with a reduction in the initial size and with an increase in the deformation rate. In addition, experimental

data indicate that the value of α for superplastic deformation is insensitive to chemical compositions: about 0.5–0.6 for some oxide materials (ZrO_2-Al_2O_3[19,35], ZrO_2-spinel-Al_2O_3[36], ZrO_2(3Y)[37] and superplastic metals (Zn-Al[33]). Such data and Eq.(5) suggest that the outline of dynamic grain-growth can be estimated from the values of k and m. It is consequently essential to suppress static grain growth by grain-boundary pinning and/or dragging. Highly limited grain growth can be expected in a microstructure consisting of three or more phases where the amount of each phase is similar. Such a multiphase structure decreases the frequency of the grain boundaries between the same phases and increases the separation distance between the phases. This situation is benefitial for suppressing grain growth, since dynamic grain growth occurs by the migration of such grain boundaries and the ripening of grains through interphase-boundary diffusion.

3 Necessary Conditions for the Occurrence of HSRS

From the discussion described in the former section, factors necessary or desirable for attaining HSRS are extracted in the first column of Table 1[23,24]. The second column summarizes the relationship between the extracted factors and superplastic deformation or cavitation. The third column indicates the dependence of these factors on processing (P), chemical compositions (C) and phases (Ph). For a given combination of chemical compositions and phases, factors (a), (b), (d) and (e) are strongly processing dependent, particularly in composites.

In Table 1, we should note that some factors appear to conflict with each other. For example, second-phase pinning is effective in suppressing dynamic grain growth, but it may act as a site of stress concentrations leading to cavity nucleation. A solution for this problem is the grain-size refinement of the second phase or of both the second and matrix phases, namely decreasing the distance that must be relaxed by diffusion (Figs.2 and 3). A minor additive that enhances diffusion may also bring about conflicting effects; the additive should simultaneously enhance stress relaxation and dynamic grain growth. The discussion about Eq.(5) indicates, however, that the weight of this problem is diminished as the

Table 1 Necessary conditions for attaining high-strain-rate superplasticity in ceramic materials

Necessary conditions	Relationship with superplastic deformation or cavitation	Note*
(a) Reduced grain size	Strain rate, stress relaxation, cavity nucleation	P, C, Ph
(b) Suppressed dynamic grain growth	Stress concentrations, cavity nucleation (second-phase pinning and dragging)	P, C, Ph
(c) Enhanced diffusivity	Strain rate, stress relaxation, cavity nucleation (aliovalent-cation doping)	C, Ph
(d) Homogeneous microstructure	Dynamic grain growth, cavity nucleation	P, Ph
(e) Reduced residual defects	Damage due to micrometer-sized cavities	P, C, Ph
(f) Low γ_b and high γ_s	Cavity nucleation (grain-boundary segregation)	C, Ph
(g) Enhanced accommodation	Cavity nucleation (glass-phase dispersion, inter-granular Si-segregation)	C, Ph

Note: * Dependence on processing (P), chemical compositions (C) and phases (Ph).

strain rate is heightened and the grain-size refinement combined with second-phase pinning may give a solution. Factors (a)–(c) and (g) of Table 1 may have been noted in studies on conventional superplasticity, whereas there have still been very limited studies that consider these factors simultaneously. The present discussion indicates that simultaneously controlling these factors is essential for attaining HSRS.

4 HSRS Attained by Microstructural Design

Paying special attention on factors (a)–(e) of Table 1, we aimed to attain HSRS in monolithic[38–40] and composite[36,41–47] materials, without using any glassy phases. We also noted that factors (a), (b), (d) and (e) are processing dependent. This is particularly the case when fine powders are used. Fine powders tend to agglomerate spontaneously owing to van der Waals forces. The agglomeration results in the formation of large pores in green bodies and sintering at a lower temperature cannot eliminate the pores. To prevent agglomeration, we applied colloidal processing[48] to fine oxide powders.

4.1 Monolithic tetragonal zirconia

For Y-TZP, since grain-growth is inherently sluggish, factors (a), (c), (d), (e) and (f) are essential for attaining HSRS. Out of these factors, we tried to control (a) and (c) through (e). Aiming at enhancing diffusion, we doped or codoped aliovalent cations using commercial high-purity powders of α-Al_2O_3[50], Mn_3O_4[39] and MgO[40]. We also used TiO_2[39], since earlier data[49] for grain growth and superplastic properties indicate that diffusion in Y-TZP is enhanced by TiO_2 addition. For the TiO_2-addition, we codoped MgO to stabilize the tetragonal phase. Using colloidal processing followed by sintering at 1300 °C for 2 h, almost fully dense materials were obtained in Al_2O_3-doped 3Y-TZP and Y-TZP codoped with TiO_2 and MgO or with Mn_3O_4 and Al_2O_3. The sintered materials consisted of a single tetragonal phase with an average grain size of 0.23 μm, where the size was defined as 1.56 times[50] the average intercept length of the grains. The examinations of sintering behavior and the rate of static grain growth confirmed the occurrence of enhanced diffusion in these materials. As shown in Fig.4, the synthesized materials exhibited HSRS at around 1400 °C and at a rate of the order of 10^{-2} s^{-1}. By the codoping of TiO_2 and MgO, the deformation temperature can be lowered to 1350 °C. This is the lowest temperature that has reported for HSRS in tension and this temperature locates in the lower limit for conventional superplasticity in Y-TZP.

4.2 Composites

In composite materials, the following merits can be expected: strongly suppressed grain growth and improved fracture strengths[51]. When Y-TZP is dispersed in the composites, transformation toughening can be expected below the transformation temperature. In spite of these merits, grain-boundary pinning may simultaneously impede grain-boundary sliding. For this reason, enhanced diffusion in the matrix and grain-size refinement are indispensable. For the latter, the elimination of agglomeration in raw materials is particularly important, since it enables us to sinter the material at a lower temperature. Of the factors listed in Table 1, we tried to control (a), (c), (d) and (e). We examined second-phase dispersion and a tri-phase structure where the volume fraction of each phase was similar. In such structures, strongly suppressed grain growth can be expected, as described before.

For a large amount of second-phase dispersion, for which clustering of the phase is unavoidable, we used such a secondary phase that itself exhibits superplastic or superplastic-like deformation. From these considerations, we synthesized materials consisting of tetragonal ZrO_2, α-Al_2O_3 and $MgO{\cdot}Al_2O_3$-spinel, where $MgO{\cdot}Al_2O_3$-spinel is expected to supply Al^{3+} and Mg^{2+} to the ZrO_2 phase and Mg^{2+} to the Al_2O_3 phase.

The synthesized materials were 30 vol. pct $MgAl_2O_4$-ZrO_2(3Y)[44–47] and 40 vol. pct ZrO_2(3Y)-30 vol. pct ($MgO{\cdot}1.1Al_2O_3$)-Al_2O_3[41–43]. For the former, colloidal processing was applied to $MgAl_2O_4$ and ZrO_2(3Y) powders. For the latter, conventional processing was applied to ZrO_2(3Y), MgO and Al_2O_3 powders. Sintering at 1400 °C for 1–2 h resulted in densified bodies with grain sizes of 0.29 μm (ZrO_2) and 0.42 μm ($MgAl_2O_4$) for the dual-phase material and 0.28 μm (ZrO_2 and spinel) and 0.45 μm (α-Al_2O_3) for the triphase material. In the triphase material the spinel phase occurred by chemical reaction between the MgO and Al_2O_3 powders. The grain size of each phase becomes smaller than that obtained by the sintering of each phase alone, particularly for the Al_2O_3 and spinel phases. The composite materials sustained noticeably high strain rates (10^{-1}–100 s^{-1}) and large tensile elongation (390%–2500%)[41–44,46]. As plotted in Fig.4, the developed monolithic and composite materials attained superplasticity at higher strain-rates than the conventional HSRS materials reported in earlier studies[1,12–15,17–20].

In the tensile data given in Fig.4, a different trend appears between the monolithic

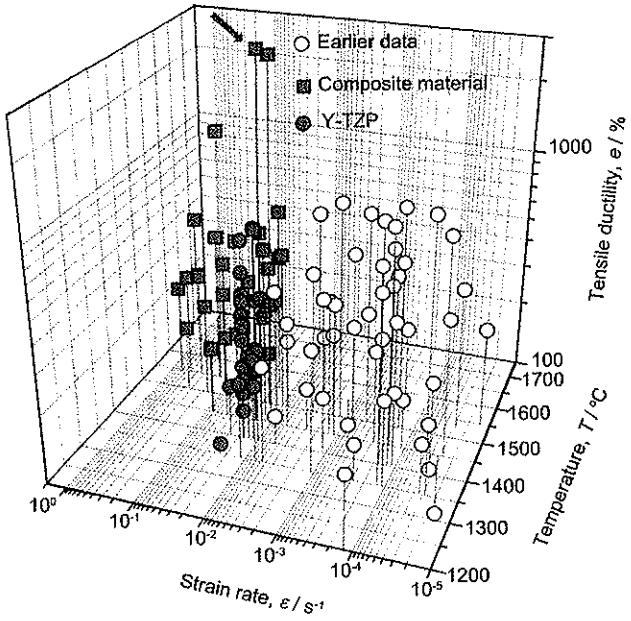

Fig.4 Tensile elongation as a function of the initial strain rate and temperature in the developed monolithic Y-TZP (•) and composite materials (■). Earlier data (○) are also plotted for comparison. The lower figure is a demonstration of large tensile ductility obserbed in a $MgO{\cdot}Al_2O_3$-spinel composite (arrowed in the upper figure).

materials and the composite materials. The former materials lie in a region of lower temperature, strain rate and tensile ductility, while the latter materials lie in a region of higher temperature, strain rate and ductility. The difference may relate to the balance among the resistance against grain growth, diffusivity and the resistance against grain-boundary sliding. Further grain-size refinement in the composites may shift the balance toward a low temperature region.

Inspection of deformed microstructure revealed some noticeable aspects in the ZrO_2[41,43] and spinel[45–47] grains: dense intragranular dislocations, dislocation-relating substructures such as subboundaries, strongly suppressed cavity formation and the sperce dispersed of cavities extremely elongated along the stress axis. These aspects indicate the enhanced relaxation of local stress concentrations that are exerted during grain-boundary sliding. To this issue, detailed discussion have been given elsewhere[23,24,37,45,53].

5 Conclusions

High-strain-rate superplasticity can be intentionally attained in doped Y-TZP and composites synthesized from ZrO_2(Y-TZP), Al_2O_3, MgO_2 and TiO_2. For this attainment, the knowledge of superplastic deformation, cavitation and dynamic grain growth emphasizes the importance of simultaneously controlling the following factors: the initial grain size, the number of residual defects, diffusivity, dynamic grain growth and the homogeneity of microstructure. For industrial application, further studies are desirable on attaining HSRS at lower temperatures and on developing high-strain-rate forming technology suitable to ceramic materials.

Acknowledgements—This work was supported by a Grant-in-Aid for Scientific Research B21360328 from JSPS and Grant-in-Aid for Scientific Research on Priority Areas 474-19053008 from MEXT, Japan.

REFERENCES

[1] F. Wakai, S. Sakaguchi and Y. Matsuno, *Adv Ceram Mater* **1(3)** (1986) 259.
[2] X. Wu and I-W. Chen, *J Am Ceram Soc* **73(3)** (1990) 746.
[3] I.A. Akmoulin, M. Djhazi, N.D. Buravova and J.J. Jonas, *Mater Sci Technol* **9(1)** (1993) 26.
[4] J. Wittenauer, *Mater Sci Forum* **243-245** (1997) 653.
[5] A. Dominguez-Rodriguez, F. Guiberteau and M. Jimenz-Melendo, *J Mater Res* **13(6)** (1998) 1631.
[6] K. Higashi, *Mater Sci Forum* **357-359** (2001) 345.
[7] M.F. Ashby and A. Verral, *Acta Metall* **21(2)** (1973) 149.
[8] R.C. Gifkins, *J Mater Sci* **13(9)** (1978) 1926.
[9] S-L. Hwang and I-W. Chen, *J Am Ceram Soc* **73(11)** (1990) 3269.
[10] A.G. Evans, J.R. Rice and J.P. Hirth, *J Am Ceram Soc* **63(7-8)** (1980) 368.
[11] H. Riedel, *Fracture at High Temperatures* (Springer-Verlag, Berlin, 1987).
[12] D.J. Schissler, A.H. Chokshi, T.G. Nieh and J. Wadsworth, *Acta Metall Mater* **39(12)** (1991) 3227.
[13] Y. Yoshizawa and T. Sakuma, *Acta Metall Mater* **40(11)** (1992) 2943.
[14] A.H. Chokshi, T.G. Nieh and J. Wadsworth, *J Am Ceram Soc* **74(4)** (1991) 869.
[15] Y. Ma and T.G. Langdon, *Acta Metall Mater* **42(8)** (1994) 2753.
[16] D.M. Owen, A.H. Chokshi and S.R. Nutt, *J Am Ceram Soc* **80(9)** (1997) 2433.
[17] K. Hiraga and K. Nakano, *Mater Sci Forum* **243-245** (1997) 387.
[18] K. Hiraga, K. Nakano, T.S. Suzuki and Y. Sakka, *Scr Mater* **39(9)** (1998) 1273.
[19] K. Hiraga, K. Nakano, T.S. Suzuki and Y. Sakka, *J Am Ceram Soc* **85(11)** (2002) 2763.
[20] K. Hiraga and K. Nakano, *Z Metallkude* **95(6)** (2004) 559.
[21] F. Wakai and H. Kato, *Adv Ceram Mater* **3(1)** (1988) 71.

[22] K.S. Chan and R.A. Page, *J Am Ceram Soc* **76(4)** (1993) 803.
[23] K. Hiraga, B-N. Kim, K. Morita, T.S. Suzuki and Y. Sakka, *J Ceram Soc Jpn* **113(3)** (2005) 191.
[24] K. Hiraga, B-N. Kim, K. Morita, H. Yoshida, T.S. Suzuki and Y. Sakka, *Sci Technol Adv Mater* **8(7-8)** (2007) 578.
[25] Y. Sakka, Y. Oishi, K. Ando and S. Morita, *J Am Ceram Soc* **74(10)** (1991) 2610.
[26] A. Kuwabara, M. Nakano, H. Yoshida, Y. Ikuhara and T. Sakuma, *Acta Mater* **52(19)** (2004) 5563.
[27] A. Kuwabara, S. Yokota, Y. Ikuhara and T. Sakuma, *Mater Trans* **45(7)** (2004) 2144.
[28] H. Yoshida, *J Ceram Soc Jpn* **114(2)** (2005) 155.
[29] K. Hiraga, K. Nakano, T.S. Suzuki and Y. Sakka, *Mater Sci Forum* **304-306** (1999) 431.
[30] W. Hancock, *Metal Sci* **10(9)** (1976) 319.
[31] M.A. Clark and T.H. Alden, *Acta Metall* **21(9)** (1973) 1195.
[32] D.S. Wilkinson and C.H. Caceres, *Acta Metall* **32(9)** (1984) 1335.
[33] O.N. Senkov and M.M. Myshlaev, *Acta Metall* **34(1)** (1986) 97.
[34] J.R. Seidensticker and M.J. Mayo, *Acta Mater* **46(14)** (1998) 4883.
[35] B-N. Kim, K. Hiraga, Y, Sakka and B-W. Ahn, *Acta Mater* **47(12)** (1999) 3433.
[36] B-N. Kim, K. Hiraga, K. Morita and Y. Sakka, *Acta Mater* **49(5)** (2001) 887.
[37] K. Morita and K. Hiraga, *Acta Mater* **50(5)** (2002) 1075.
[38] T.S. Suzuki, Y. Sakka, K. Morita and K. Hiraga, *Scr Mater* **43(8)** (2000) 705.
[39] Y. Sakka, T. S. Suzuki, K. Morita, B-N. Kim, K. Hiraga and Y. Moriyoshi, *Adv Eng Mater* **5(3)** (2003) 130.
[40] Y. Sakka, T. Ishii, T.S. Suzuki, K. Morita and K. Hiraga, *J Euro Ceram Soc* **24(1-4)** (2004) 449.
[41] B-N. Kim, K. Hiraga, K. Morita and Y. Sakka, *Nature* **413(6853)** (2001) 288.
[42] B-N. Kim, K. Hiraga, K. Morita, Y. Sakka and T. Yamada, *Scr Mater* **47(11)** (2002) 775.
[43] B-N. Kim, K. Hiraga and K. Morita, *Mater Sci Forum* **426-432** (2003) 2729.
[44] K. Morita, K. Hiraga and Y. Sakka, *J Am Ceram Soc* **85(7)** (2002) 1900.
[45] K. Morita, K. Hiraga, B-N. Kim and Y. Sakka, *Philos Mag Lett* **83(9)** (2003) 533.
[46] K. Morita, K. Hiraga, B-N. Kim and Y. Sakka, *Mater Trans* **45(7)** (2004) 2073.
[47] K. Morita, K. Hiraga, B-N. Kim and Y. Sakka, *Mater Sci Forum* **475-479** (2005) 2977.
[48] J. Cesarano III, L.A. Aksay and A.J. Bleier, *J Am Ceram* **71(4)** (1988) 250.
[49] K. Tsurui and T. Sakuma, *Scr Mater* **34(3)** (1996) 443.
[50] M.I. Mendelson, *J Am Ceram Soc* **52(8)** (1969) 443.
[51] M.P. Harmer, H.M. Chan and J. Miller, *J Am Ceram Soc* **75(7)** (1992) 1715.
[52] K. Hiraga, *J Ceram Soc Jpn* **115(6)** (2007) 395.